
This is the **submitted version** of the journal article:

Giordano, Andrea; Santo Domingo, Miguel; Quadrana, Leandro; [et al.].
«CRISPR». *Journal of Experimental Botany*, Vol. 73, Issue 12 (June 2022), p.
4022-4033. DOI 10.1093/jxb/erac148

This version is available at <https://ddd.uab.cat/record/259589>

under the terms of the  IN COPYRIGHT license

1
2 **CRISPR/Cas9 gene editing uncovers the role of CTR1 and ROS1 in melon**
3 **fruit ripening and epigenetic regulation**

4 Andrea Giordano^{1*}, Miguel Santo Domingo¹, Leandro Quadrana³,
5 Marta Pujol^{1,2}, Ana Montserrat Martín-Hernández^{1,2} and Jordi Garcia-Mas^{1,2*}

6 ¹Centre for Research in Agricultural Genomics (CRAG) CSIC-IRTA-UAB-UB, Edifici CRAG, Campus UAB,
7 08193 Bellaterra, Barcelona, Spain.

8 ²Institut de Recerca i Tecnologia Agroalimentàries (IRTA), Edifici CRAG, Campus UAB, 08193 Bellaterra,
9 Barcelona, Spain.

10 ³Institut de Biologie de l'Ecole Normale Supérieure, Paris, France.

11 Andrea Giordano: andrea.giordano@cragenomica.es

12 Miguel Santo Domingo: miguel.santodomingo@cragenomica.es

13 Leandro Quadrana: leandro.quadrana@bio.ens.psl.eu

14 Marta Pujol: marta.pujol@irta.cat

15 Ana Montserrat Martín-Hernández: montse.martin@irta.cat

16 Jordi Garcia-Mas: jordi.garcia@irta.cat

17 *Corresponding author:

18 Jordi Garcia-Mas, jordi.garcia@irta.cat, Phone: +34 935636600

19 Andrea Giordano, andrea.giordano@cragenomica.es, Phone: +34 935636600

21 **Date of submission: 31/01/2022**

22 **Number of tables: 0**

23 **Number of figures: 4**

24 **Word count: 3542**

25 **Number of supplementary Tables: 6**

26 **Number of supplementary Figures: 5**

27 **Running title: Gene editing of two key players in melon ripening**

28

29

30

31

32

33

34

35

36

37

38

39

40

41

42

43

44

45

46 **Highlight**

47

48 *CmROS1* and *CmCTR1-like* CRISPR/Cas9 mutants accelerate fruit ripening in
49 melon. Besides, *CmROS1* contributes to maintain the methylation levels along
50 fruit ripening by hypomethylation of ripening genes.

51

52

53 **Abstract**

54

55 Melon (*Cucumis melo* L.) has emerged as an alternative model to study fruit
56 ripening due to the coexistence of climacteric and non-climacteric varieties.
57 The previous characterization of a major QTL *ETHQV8.1* sufficient to trigger
58 climacteric ripening in a non-climacteric background allowed the identification
59 within the QTL interval of a negative regulator of ripening *CmCTR1-like*
60 (MELO3C024518), and a putative DNA demethylase *CmROS1*
61 (MELO3C024516), the orthologue of *DML2*, a DNA demethylase regulating fruit
62 ripening in tomato. To understand the role of these genes in climacteric
63 ripening, we generated homozygous CRISPR knockout mutants of *CmCTR1-*
64 like and *CmROS1* in a climacteric genetic background. The climacteric behavior
65 was altered in both loss-of-function mutants in two summer seasons with an
66 advanced ethylene production profile compared to the climacteric wild type,
67 suggesting a role of both genes in climacteric ripening in melon. Single cytosine
68 methylome analyses of the *CmROS1* knockout mutant revealed DNA
69 methylation changes in the promoter regions of key ripening genes as *ACS1*,
70 *ETR1* and *ACO1*, and ripening associated-transcription factors as *NAC-NOR*,
71 *RIN* and *CNR*, suggesting the importance of *CmROS1*-mediated DNA
72 demethylation for triggering fruit ripening in melon.

73 **Keywords:** fruit ripening, CRISPR, melon, cucurbits

74 **Introduction**

75

76 During the ripening process, fleshy fruits undergo physiological and metabolic
77 changes affecting color, flavor, firmness, and aroma. These changes are driven
78 by phytohormones and developmental factors and occur in a highly coordinated
79 manner with a direct impact on fruit quality and shelf-life (Giovannoni, 2001).
80 One of the main promoters of fruit ripening is the volatile hormone ethylene.
81 Depending on the involvement of this hormone during ripening, fruits have been
82 traditionally divided into i) climacteric, characterized by an increase in

83 respiration and ethylene production at the onset of ripening and ii) non
84 climacteric, presenting low levels of both ethylene production and respiration
85 rate across the process (McMurchie *et al.*, 1972). Dissecting the regulatory
86 network underlying the control of fruit ripening has been a major goal due to its
87 biological significance but also for its commercial value (Giovannoni *et al.*, 2017;
88 Wang *et al.*, 2020).

89 Important advances in the understanding of the molecular mechanisms
90 underlying climacteric fruit ripening have been made in the model species
91 tomato (Giovannoni, 2007). Ripening related mutants allowed the identification
92 of several transcription factors that are upstream regulators of ethylene
93 dependent or independent ripening. Among them *RIPENING INHIBITOR (RIN)*,
94 *NON-RIPENING (NOR)*, and *COLORLESS NON-RIPENING (CNR)* (Vrebalov
95 *et al.*, 2002; Manning *et al.*, 2006; Giovannoni, 2007).

96 Recent studies demonstrated that DNA methylation levels play an important
97 role at the onset of fruit ripening in tomato (Zhong *et al.*, 2013). Moreover, the
98 DNA methylation dynamics in a climacteric and an ethylene repressed line have
99 been recently studied in melon (Feder *et al.*, 2020). Modulation of DNA
100 methylation levels is governed by DNA methylases and demethylases. The
101 enzymatic removal of methylcytosine in plants is initiated by a family of DNA
102 glycosylases/lyases, including DEMETER (DME), Repressor of silencing 1
103 (ROS1), DEMETER-like2 (DML2) and DEMETER-like3 (DML3), firstly
104 characterized in the model plant *Arabidopsis thaliana* (Zhu, 2009). In tomato,
105 SIDML2 is induced upon the onset of ripening leading to a global DNA
106 hypomethylation during ripening (Zhong *et al.*, 2013; Liu *et al.*, 2015; Lang *et*
107 *al.*, 2017). Knockout using CRISPR/Cas9 system and knockdown RNAi mutants
108 in this species revealed that *SIDML2* is required for normal fruit ripening by the
109 activation of ripening-induced genes and repression of several ripening-
110 repressed genes (Zhong *et al.*, 2013; Lang *et al.*, 2017). Nonetheless, the
111 tomato model is not universal as different transcriptional positive feedback
112 circuits controlling ripening in climacteric species were identified (Lü *et al.*,
113 2018).

114 Melon (*Cucumis melo* L.) has emerged as an alternative model to study fruit
115 ripening since both climacteric (e.g. *cantalupensis* types as 'Védrantais' (VED))
116 and non-climacteric (e.g. *inodorus* types as 'Piel de Sapo' (PS)) genotypes

117 exist. The recent characterization of a major QTL in chromosome 8 of melon,
118 *ETHQV8.1*, which is sufficient to activate climacteric ripening in a non-
119 climacteric background, allowed the identification of candidate genes related to
120 fruit ripening in a genomic interval of 150 kb that contained 14 annotated genes
121 (Pereira *et al.*, 2020). Some of these genes are highly expressed in fruits and
122 contain multiple non-synonymous polymorphisms distinguishing the climacteric
123 VED from the non-climacteric PS genotype.

124 One of the candidates (*CmROS1*, MELO3C024516) encodes the homolog of
125 the main DNA demethylase *ROS1* in *Arabidopsis*, which targets mainly
126 transposable element (TE) sequences and regulates some genes involved in
127 pathogen response and epidermal cell organization (Yamamuro *et al.*, 2014; Le
128 *et al.*, 2014). The closest orthologue in tomato, *SIDML2* is crucial for the DNA
129 demethylation of fruit ripening genes including ethylene synthesis and signaling
130 (Lang *et al.*, 2017).

131 The other candidate gene is *CONSTITUTIVE TRIPLE RESPONSE 1* (*CTR1*) a
132 serine/threonine kinase (*CmCTR1*-like, MELO3C024518). This kinase interacts
133 physically with ethylene receptors as a negative regulator of the ethylene signal
134 transduction pathway (Kieber *et al.*, 1993). In the absence of ethylene, *CTR1* is
135 activated, preventing the downstream transduction pathway; when ethylene is
136 present, the ethylene receptor terminates the activation of *CTR1*, leading to the
137 ethylene responses (Binder, 2008). In tomato, the silencing of *CTR1* promoted
138 fruit ripening, validating its role as a negative regulator of the ethylene signal
139 transduction pathway (Fu *et al.*, 2005).

140 In this study, we aimed to better understand the role of the two *ETHQV8.1*-
141 containing candidate genes *CmROS1* and *CmCTR1*-like in fruit ripening by
142 obtaining CRISPR/Cas9-induced loss-of-function mutants in a climacteric melon
143 genotype. Furthermore, we characterized the role of *CmROS1* in DNA
144 methylation homeostasis during fruit ripening.

145 **Materials and methods**

146 **CRISPR/Cas9 vector Construction**

147 To target *CmROS1* (MELO3C024516) two different guide RNAs (gRNA) of 20
148 nucleotides in length separated by 188 bp were designed using Breaking Cas

149 tool (<https://bioinfogp.cnb.csic.es/tools/breakingcas/>) (Table S1). The two
150 oligonucleotides generated for each gRNA were annealed and cloned in the
151 sites *BbsI* and *BsaI* into the plasmid p-tandemgRNA. The construct was verified
152 by sequencing and then digested with *SphI* and *KpnI* to release the cassette
153 that was then inserted into the same sites in the pB7-Cas9-TPC-polylinker
154 binary vector. Cloning vectors were kindly provided by Prof. Puchta (KIT,
155 Germany).

156 For *CmCTR1*-like (MELO3C024518) we used the pEn-CHIMERA vector
157 provided by Prof. Puchta (KIT, Germany) to generate the entry construct. A
158 single gRNA of 20 nucleotides was designed using Breaking Cas tool
159 (<https://bioinfogp.cnb.csic.es/tools/breakingcas/>) (Table S1). Cloning steps of
160 the gRNA and transfer to the pDe-Cas9 binary vector were performed as
161 previously described (Schiml and Puchta, 2016).

162 **Agrobacterium mediated plant transformation**

163
164 *Agrobacterium tumefaciens* (strain AGL-0) cells were transformed with the
165 binary CRISPR/Cas9 constructs. Plant transformation was performed by co-
166 cultivation of the Agrobacterium culture with one-day-old cotyledons of VED as
167 previously described (Castelblanque *et al.*, 2008), except that cotyledons were
168 dissected as in (García-Almodóvar *et al.*, 2017). In brief, seeds were peeled and
169 incubated for one day in germination MS medium. Then, the embryo was
170 removed from the cotyledons and the half proximal part was incubated with the
171 Agrobacterium culture for 20 minutes in the presence of 200 µM
172 acetosyringone. After incubation, Agrobacterium was co-cultured with the
173 explants during three days at 28 °C in the regeneration medium (Castelblanque
174 *et al.*, 2008) supplemented with 0,5 mg/L 6-bencylaminopurine (BA), 0,1 mg/L
175 Indole-3-acetic acid (IAA) and 200 µM acetosyringone. Every three weeks, calli
176 were cleaned and the green buds were selected and replicated in fresh
177 regeneration media without acetosyringone and supplemented with L-
178 Phosphinothricin (PPT) for selection. Selected transgenic plants containing the
179 *bar* gene were grown in a growth room under a 12-h light/12-h dark cycle at 28
180 °C. After two to four months, individual transgenic plants were transferred to
181 rooting medium (regeneration medium without hormones).

182

183 **Detection of mutations**

184 Genomic DNA from leaves of in vitro plantlets (T0) and from young leaves of T1
185 and T2 plants was extracted using the CTAB method with some modifications
186 as described in (Pereira *et al.*, 2018). The transgene presence was detected by
187 PCR using specific primers targeting Cas9. Genomic regions flanking gRNA1
188 and gRNA2 of *CmROS1* were amplified by PCR using specific primers. For
189 detection of mutations in *CmCTR1*-like, a region targeting the gRNA was
190 amplified with specific primers. All primers are listed in Table S2. Mutations
191 were detected by sequencing the amplified fragments and identified by double
192 peaks in the sequence chromatograms. Purified PCR products were cloned into
193 p-Blunt II-TOPO vector (Life Technologies) and sequencing of colonies using
194 M13F and M13R primers was performed to confirm the mutations.

195

196 **Generation of T2 plants and phenotyping of climacteric ripening traits**

197 Ploidy level of T0 plants was evaluated by flow-cytometry analysis and selected
198 T0 plants for each gene were grown under greenhouse conditions (25°C for 16
199 hours and 22°C for 8 hours) and self-pollinated. T1 seedlings were screened for
200 the presence of Cas9 by PCR. After segregation, non-transgenic homozygous
201 edited T1 plants were selected and grown under greenhouse conditions to
202 obtain the T2 seeds for the phenotypic assay.

203 Edited T2 *CmROS1* (n=8) and *CmCTR1*-like plants (n=8) were grown
204 randomized under greenhouse conditions (24°C for 16 hours and 22°C for 8
205 hours) at Caldes de Montbui (Barcelona) in 2020 and 2021. VED plants were
206 used as a wild type control plant (n=8). Plants were weekly pruned and
207 manually pollinated to obtain one fruit per plant. The harvest date was
208 determined following two criteria: either abscission date, when the fruit abscised
209 from the plant, or 5 days after the formation of the abscission layer when it was
210 not complete.

211 Ripening-related traits were evaluated as described in Pereira *et al.* 2020 in two
212 consecutive summer seasons (2020 and 2021). Production of aroma (ARO),

213 chlorophyll degradation (CD) and abscission layer formation in the pedicel of
214 the fruit (ABS) were daily evaluated and firmness was measured at harvest
215 time. The visual inspection of melon fruits, attached to the plant, was performed
216 daily, from approximately 20 days after pollination (DAP) until harvest. In
217 addition, individual pictures of the fruits were obtained weekly. ARO, ABS and
218 CD were recorded as 0 = absence and 1 = presence. The aroma production
219 was evaluated every day by smelling the fruits. The firmness of fruit flesh was
220 measured at harvest using a penetrometer (Fruit TestTM, Wagner Instruments),
221 in at least three regions of the fruit (distal, proximal and median), and the mean
222 value was registered.

223 **Ethylene production**

224 Ethylene production *in planta* was measured in the 2020 summer season using
225 non-invasive gas chromatography – mass spectrometry (GC-MS) method, as
226 described in (Pereira *et al.*, 2017). The ethylene peak was monitored before
227 ripening from 20 DAP until harvest. The atmosphere of the chamber containing
228 the fruit was measured every day.

229 The ethylene peak was characterized by four traits, measured as described in
230 Pereira *et al.*, 2020: maximum production of ethylene in the peak (ETH),
231 earliness of ethylene production (DAPE), earliness of the ethylene peak
232 (DAPP), and width of ethylene peak (WEP).

233 **Epigenomics**

234 DNA was extracted from fruit flesh of ROS1-CRISPR-2 and the wild-type VED
235 at different ripening stages (15, 25 and 30 DAP and harvest point) following the
236 CTAB protocol (Doyle and JJ, 1990) adding a purification step using
237 Phenol:Chloroform:Isoamyl alcohol (25:24:1). For each time point, three
238 biological replicates were analysed. Bisulfite conversion, BS-seq libraries and
239 sequencing (paired-end 100 nt reads) were performed by BGI Tech Solutions
240 (Hong Kong). Mapping was performed on melon genome v3.6.1 (Ruggieri *et*
241 *al.*, 2018) using Bismark v0.14.2 (Krueger and Andrews, 2011) and the
242 parameters: --bowtie2, -N 1, -p 3 (alignment); --ignore 5 --ignore_r2 5 --
243 ignore_3prime_r2 1 (methylation extractor). Only unique mapping reads were

244 retained. The methylKit package v0.9.4 (Akalin *et al.*, 2012) was used to
245 calculate differential methylation in 100 bp non-overlapping windows (DMRs).
246 Significance of calculated differences was determined using Fisher's exact test
247 and Benjamin-Hochberg (BH) adjustment of p-values (FDR<0.05) and
248 methylation difference cutoffs of 40% for CG, 20% for CHG and 20% for CHH.
249 Differentially methylated windows within 100 bp of each other were merged to
250 form larger DMRs. 100 bp windows with at least six cytosines covered by a
251 minimum of six (CG and CHG) and ten (CHH) reads per comparison were
252 considered.

253

254 **Statistical analyses**

255 All the statistical analyses and graphical representations were obtained using
256 the software R v3.2.3 (R Core Team, 2020) with the RStudio v1.0.143 interface
257 (RStudio: Integrated development environment for R, 2012).

258

259 **Results**

260

261 **Generation of CRISPR/Cas9 knockout mutants in candidate genes for** 262 ***ETHQV8.1* and inheritance of the editions**

263

264 To investigate the role of *CmROS1* (MELO3C024516) and *CmCTR1*-like
265 (MELO3C024518) genes in the fruit ripening process in melon, we knocked
266 them out using the CRISPR/Cas9 gene editing system in a climacteric genetic
267 background (VED).

268 A strategy with two target sites in exon 2 was used for *CmROS1* (Fig. 1). We
269 obtained 15% transformation efficiency, recovering in total 59 transgenic rooted
270 plants. From the transgenic plants, almost half of them (46%) were edited.
271 Multiple independent transgenic plants were genotyped by sequencing the
272 genomic DNA spanning both target sites. Most of the editions (75%) occurred in
273 target 1 (gRNA1) whereas only a few editions (25%) were obtained for target 2
274 (gRNA2). Several different insertions and deletions were obtained in T0 plants
275 with biallelic or heterozygous mutations (Fig. S1), with several plants carrying
276 the same mutation (+1 bp). A diploid biallelic line with an insertion of 1 bp and a
277 deletion of 23 bp that were predicted to generate truncated proteins was
278 selected for further work (Fig. 1A).

279 The selected biallelic T0 line was self-pollinated to obtain non-transgenic (Cas9
280 free) plants carrying homozygous editions. After segregation, T1 lines
281 homozygous for the 1 bp insertion (ROS1-CRISPR-1) or the 23 bp deletion
282 (ROS1-CRISPR-2) were selected for further study (Fig. 1A and C).
283 A different CRISPR Cas9 strategy was used to target the *CmCTR1*-like gene. A
284 single target site was selected in exon 6 of *CmCTR1*-like (Fig. 1B). For this
285 target gene we obtained 12% of transformation efficiency. Transgenic T0 plants
286 were screened for mutations in the target site and 40% were edited showing
287 mainly large or small deletions (Fig. S1). From the edited T0 plants, a biallelic
288 line carrying a 11 bp deletion and a 1 bp insertion was selected and self-
289 pollinated to segregate out the Cas9 transgene. The genetic editions were
290 stably transmitted to T1 plants. After segregation, a homozygous edited line
291 carrying the 11 bp deletion (CTR1-CRISPR-1), which is predicted to generate a
292 premature termination codon, and the homozygous line with 1 bp insertion
293 (CTR1-CRISPR-2), generating a frame shift, were grown under greenhouse
294 conditions for the characterization of fruit ripening related traits (Fig. 1B and C).
295

296 ***CmROS1* and *CmCTR1*-like edited plants show altered ripening 297 phenotypes**

298 ROS1-CRISPR-1/2 and CTR1-CRISPR-1/2 were evaluated and characterized
299 for ripening related traits in two consecutive summer seasons (2020 and 2021).
300 However, the line CTR1-CRISPR-2 was only characterized in 2021 due to a
301 powdery mildew infection of some replicates in 2020 that prevented its
302 evaluation. Overall, the fruit appearance (shape, weight and colour) of the
303 CRISPR edited lines did not show major differences with the wild-type VED at
304 harvest time and no significant changes were detected in the flesh firmness
305 (Fig. 1C, Table S3). To better characterize the ripening process, we measured
306 ethylene production *in planta* in 2020 with a non-invasive methodology allowing
307 observing the phenotype of the downstream effects of this hormone.
308 The phenotypic characterization revealed a significant earliness of the
309 climacteric symptoms for all the edited lines showing the same ripening
310 behavior pattern in both years (Fig. 2, Table S3). In 2020, the earliest
311 climacteric symptom was sweet aroma production (EARO), which in the
312 CRISPR edited lines for both genes appeared around two days before VED.

313 The initiation of the rind color change, which is attributed to chlorophyll
314 degradation (ECD), was appreciated almost simultaneously with the detection
315 of the abscission layer formation (EALF) and both ripening-related traits arose
316 in both *CmROS1* edited lines two days before VED. The CTR1-CRISPR-1
317 edited line exhibited the earliness of the ripening related traits all at the same
318 time, which differed significantly from VED, arising around three days before
319 than VED for ECD and EALF and two days for EARO.

320 During the second summer season, we evaluated all the CRISPR edited lines.
321 In general, the environmental conditions delayed ripening of both VED and
322 mutant plants (around 4-5 days later in 2021). Despite this environmental effect,
323 all CRISPR edited lines displayed significant advances of about three days in
324 the ripening-related traits ECD, EARO and EALF when compared to VED (Fig.
325 2). Moreover, during this year, the line CTR1-CRISPR-2 was evaluated, and
326 the dataset showed the same behavior for both CTR1-like edited lines. ROS1
327 edited lines also showed the same pattern between them.

328 We also monitored fruit ethylene emission daily in 2020 without altering the
329 ripening process (Fig. 2C). The CRISPR edited lines showed a different
330 ethylene production pattern compared to wild-type VED, with both *CmROS1*
331 edited lines showing the same profile. In *CmROS1* mutant lines, ethylene
332 production started two days before the wild-type VED and with an increment of
333 2.7 to 3-fold of ethylene production (Fig. 2C and Table S3).

334 For *CmCTR1*-like edited lines, ethylene measurements for CTR1-CRISPR-2
335 were not available due to the infection with powdery mildew of some of the
336 replicates of this line at around 20 DAP. The CTR1-CRISPR1 line showed a
337 significant difference in the earliness of ethylene production (DAPE) and
338 earliness of ethylene peak (DAPP). In this line, ethylene was detected around
339 three days in advance of wild-type VED. Similarly, the peak of ethylene
340 production was also advanced three days in CTR1-CRISPR1 compared to wild-
341 type VED. However, this advancement was not accompanied by a significant
342 difference in the maximum quantity of ethylene produced (Fig. 2C and Table
343 S3). Overall, these results demonstrate that both candidate genes are involved
344 in melon fruit ripening.

345

346 **Characterization of the ROS1-CRISPR and VED methylome at different**
347 **fruit ripening stages**

348

349 To better understand at the molecular level the role of *CmROS1* in DNA
350 demethylation and fruit ripening in melon, we generated single-cytosine
351 resolution methylomes by whole genome bisulfite sequencing from fruits of
352 ROS1-CRISPR-2 and the wild-type VED plants at 15, 25 and 30 DAP as well as
353 at harvest (H) point (Fig. 3A).

354 When comparing the global methylation level along ripening in VED, we found
355 that methylation at CG and CHG contexts declines along fruit ripening, showing
356 around 2,000 and 4,000 hypomethylated regions (DMR), versus 300 and 3,000
357 hypermethylated regions in the CG and CHG context, respectively, at harvest
358 time compared to the first stage of ripening (i.e. H vs 15 DAP) (Fig. 3B).
359 Interestingly, these changes were more often associated with promoter and
360 intergenic regions (Fig. 3D).

361 In order to evaluate the role of *CmROS1* in the observed DNA methylation
362 dynamics, we compared the methylation level in the three contexts of ROS1-
363 CRISPR-2 and the wild-type VED plants at the same ripening stage (Fig. 3C). In
364 this way, we identified numerous changes in DNA methylation levels for the
365 three sequence contexts. In total (CG, CHG and CHH context together), we
366 found 16,968 hypermethylated DMRs at 15 DAP, 26,497 at 25 DAP, 19,928 at
367 30 DAP and 43,156 at H time relative to VED, while the total hypomethylated
368 DMRs were 23,742 at 15 DAP, 36,813 at 25 DAP, 24,083 at 30 DAP and
369 33,698 at H time. Overall, CRISPR-ROS1 line is associated with
370 hypomethylation of CG and hypermethylation of CHG DMRs (Fig. 3C).

371 To further investigate the targets of ROS1 we focused on the hypermethylated
372 DMRs in the CRISPR-ROS1 line (Table S4). Moreover, in CHH context at H
373 time there are changes in the number of DMRs annotation between VED and
374 the edited line. Among the CHH hypermethylated regions in CRISPR-ROS1
375 compared to VED at H time, 14% are associated with TEs, 46% with intergenic
376 regions, 6% in promoter regions (defined as 1 kb upstream transcriptional start
377 sites), and 33% in genic regions (Fig. 3D).

378 Notably, Gene ontology (GO) enrichment analysis of genes associated with
379 hypermethylated DMRs at H time in the CRISPR-ROS line compared to VED
380 and hypomethylated along ripening in VED context revealed an

381 overrepresentation of genes related to response to stress in CRISPR-ROS1
382 compared to VED (Table S5).

383 **CmROS1 targets promoter regions of key genes involved in ripening**

384 We have further analysed the methylation level of key genes known to
385 participate in the ripening process in the three contexts. Changes were found at
386 different stages of ripening in the promoter region of genes involved in the
387 ethylene biosynthesis or signaling pathway: *ACS1* (MELO3C016340.2), *ETR1*
388 (MELO3C003906.2) and *ACO1* (MELO3C014437) as well as in ripening
389 associated-transcription factors: *NAC-NOR* (MELO3C016540), *RIN*
390 (MELO3C026300.2) and *CNR* (MELO3C002618.2) (Fig. 4).

391 Notably, the promoter region of *ACS1* appeared hypomethylated on the three
392 sequence contexts in the CRISPR-ROS1 line compared to VED in all the time
393 points studied along ripening. Furthermore, hypomethylation of the *ACO1*
394 promoter (CG and CHH context) was observed at 25 and 30 DAP and the *ETR1*
395 promoter region (CHG and CHH context) at 30 DAP. In contrast, CHG
396 hypermethylation of *NAC-NOR* was found from the earliest stage until 30 DAP
397 in the mutant and was hypomethylated at 30 DAP in the CHH context. For the
398 other two transcription factors, we observed CHH hypomethylation of *RIN* and
399 *CNR* promoter regions at H time. These results suggest that *CmROS1* plays a
400 role in the complex modulation of DNA methylation levels of promoter regions of
401 important genes involved in ripening.

402

403 **Discussion**

404 Advances in genome editing have been obtained applying the CRISPR/Cas
405 technology in several plant species. However, among the Cucurbitaceae family
406 studies were only reported in watermelon for herbicide resistance (Tian *et al.*,
407 2016, 2018) and cucumber for virus resistance (Chandrasekaran *et al.*, 2016).
408 More recently, edited plantlets with a disruption of a visual reporter gene
409 (*CmPDS*), which could not be carried to the next generation, were generated in
410 melon using CRISPR/Cas9 (Hooghvorst *et al.*, 2019). To our knowledge,
411 hereby we report for the first time the generation of melon knockout mutants for
412 an agronomic important trait such as fruit ripening and the inheritance of the
413 introduced mutations to the following generations using CRISPR/Cas9.

414 Melon is considered a recalcitrant species for genetic transformation. In this
415 study, we obtained on average 15% transgenic plants and from these, 40% and
416 46% of them were successfully edited plants for our target genes *CmROS1* and
417 *CmCTR1*-like using either two or one gRNA strategy, respectively. The edited
418 plants carried several types of editions nearby the protospacer adjacent motif
419 (PAM) sequence of the target gRNA. As reported for other species (Feng *et al.*,
420 2014), biallelic edited plants were obtained (70% of the edited plants),
421 suggesting early editions during developmental stages.

422 In accordance with the mutations induced by Non-homologous end Joining
423 pathway, the sequence analysis of the edited lines revealed that the most
424 frequent editions were insertions and deletions with more than one independent
425 event exhibiting the same edition. All the gRNA used here successfully induced
426 mutations in the target genes. However, editions in *CmROS1* were mainly
427 obtained in gRNA1 suggesting a higher edition efficiency for this gRNA. In
428 addition, in contrast to the observations reported by Hooghvorst *et. al.*, base
429 pair substitutions were not obtained for any of the genes targeted in this study.

430 The improvements in the transformation protocol of melon allowed setting up an
431 efficient method to obtain transgenic plants in a recalcitrant species and hence,
432 increased the chances to obtain edited plants. On the other hand, according to
433 our results, the efficiency of the gRNA determines the rate of success of edited
434 lines on the target genes used in this work. Thus, testing the efficiency of the
435 gRNA before transformation could be a key step for gene editing in this species.

436 Improving fruit quality and shelf life has been one of the main challenges for
437 agriculture. During the last decades, advances in understanding the ripening
438 process were approached by conventional breeding and genetic engineering
439 tools. For instance, CRISPR knockout mutants in tomato have proved the
440 importance of master ripening regulator genes (Ito *et al.*, 2015).

441 More recent studies showed that epigenetic regulation plays a key role in fruit
442 ripening with both hypermethylated and hypomethylated loci for several species
443 (Lü *et al.*, 2018). The balance of global DNA methylation/demethylation is
444 altered during fruit ripening and these alterations are governed by DNA
445 demethylases. In tomato, more than 200 promoters of ripening-related genes,
446 including master regulators, ethylene related genes, fruit softening, and

447 carotenoids synthesis genes, are regulated by DNA demethylation at the onset
448 of ripening (Zhong *et al.*, 2013).

449 In *Arabidopsis*, the protein repressor of silencing 1 (*ROS1*), which belongs to
450 the subfamily of bifunctional 5-methylcytosine DNA glycosylases/lyases, has
451 been characterized as the main sporophytic DNA demethylase (Gong *et al.*,
452 2002). In tomato, there are four genes (*SIDML1*, *SIDML2*, *SIDML3* and *SIDML4*)
453 encoding putative DNA demethylases, being *SIDML2* the closest ortholog to
454 *Arabidopsis ROS1* gene. Furthermore, *SIDML2* expression is highly correlated
455 with fruit ripening (Zhong *et al.*, 2013; Liu *et al.*, 2015). In melon, we have
456 identified four putative *ROS1* homologues (MELO3C024516, MELO3C021451,
457 MELO3C002241 and MELO3C009432) (Fig. S2). The gene MELO3C024516
458 locates in the previously identified ripening QTL interval *ETHQV8.1* (Table S6)
459 and therefore was edited in this study. The CRISPR-ROS1/2 lines, carrying
460 loss-of-function homozygous alleles of MELO3C024516, showed an advance in
461 climacteric ripening compared to the wild type, suggesting a role of this gene in
462 the complex regulation of climacteric ripening in melon. Interestingly, RNA-seq
463 expression analysis of several fruit ripening stages in wild type climacteric VED
464 shows that the four putative *ROS1* genes have a similar expression profile
465 along ripening (Fig. S3), suggesting that more than one DNA demethylase may
466 be involved in this process. Moreover, a recent study showed hypomethylation
467 of ethylene induced genes at 30 DAP in a climacteric variety, suggesting the
468 important role of DNA demethylases during melon ripening (Feder *et al.*, 2020).
469 Unlike in tomato, in which the CRISPR *SIDML2* mutant showed an inhibitory
470 effect on fruit ripening (Lang *et al.*, 2017), the *CmROS1* knockout melon fruit
471 ripens ahead of the wild type VED.

472 Our methylome analysis of the climacteric variety VED showed an overall
473 demethylation in CG and CHG context along fruit ripening, similar to what has
474 been reported in tomato (Liu *et al.*, 2015; Lang *et al.*, 2017), orange (Huang *et*
475 *al.*, 2019) and strawberry (Cheng *et al.*, 2018).

476 The asymmetry in the relative number of statistically significant hypermethylated
477 and hypomethylated DMRs between VED and ROS1-CRISPR-2, lead to an
478 overall hypomethylation of CG and hypermethylation of CHG in the ROS1
479 CRISPR mutant. Both hyper and hypo- methylated loci were also reported in
480 *Arabidopsis ros1* mutants (Penterman *et al.*, 2007). Furthermore,

481 hypomethylation levels in the promoter regions of key ripening genes (e.g.
482 *ACS1*, *ETR1*, *ACO1*) are in agreement with the phenotype displayed by the
483 *CmROS1* CRISPR lines. The expression level of these genes and other DMRs
484 involved in ethylene signaling and ripening needs to be further studied to
485 provide insights into ripening regulation in melon. In addition, in our study,
486 genes related to biotic stress response were also hypomethylated in *ROS1* vs
487 *VED* at harvest, suggesting a possible role of this DNA demethylase in stress-
488 response genes, as reported for *ROS1*, *DML2*, *DML3* in response to biotic
489 stress in *Arabidopsis* (Le *et al.*, 2014; Halter *et al.*, 2021).

490 Both mutant lines of *CTR1*-CRISPR promote fruit ripening in melon in
491 agreement to the phenotype described when silencing *LeCTR1* in tomato fruits
492 (Fu *et al.*, 2005) and the previously described role of *CTR1* as a negative
493 regulator of ethylene signaling in other species (Binder, 2008). This second
494 candidate gene of the QTL *ETHQV8.1* (Table S6) is closely related to *CTR1* in
495 other species (Fig. S4) and is differentially expressed at harvest between a non-
496 climacteric and a climacteric variety (Fig. S5). Our study shows that *CmCTR1*-
497 like plays also an important role in the ripening process as a negative regulator
498 affecting the initiation of the ripening process but without affecting other
499 important traits such as firmness.

500 To our knowledge, this is the first time that the CRISPR technology has been
501 implemented on genes involved in agronomically important traits in melon. The
502 implementation of this technology in this species and the inheritance of the
503 editions to the following generations is of high interest and a valuable resource
504 not only for researchers but also for breeders. We have functionally validated
505 two genes involved in the complex regulation of fruit ripening and studied in
506 depth the role of the DNA demethylase *ROS1* in fruit ripening. However, as
507 mutants for both candidate genes *CmROS1* and *CmCTR1*-like showed an
508 altered ripening phenotype, further studies are needed to identify which of them
509 is the candidate for *ETHQV8.1*.

510

511 **Supplementary Data**

512 **Supplementary Tables:**

513 Supplementary Table 1: List of gRNAs to target *CmROS1* and *CmCTR1-like*
514 genes.
515 Supplementary Table 2: List of primers to detect Cas9 and mutations in
516 CRISPR lines.
517 Supplementary Table 3: Climacteric ripening related traits in two consecutive
518 summer seasons.
519 Supplementary Table 4: DMRs hypermethylated in ROS line compared to VED
520 at harvest time
521 Supplementary Table 5: GO of target genes at harvest time
522 Supplementary Table 6: List of potential candidate genes for *ETHQV8.1*.

523 **Supplementary Figures:**

524 Supplementary Figure 1: Editions obtained for *ROS1* and *CmCTR1-like* in T0
525 melon plants.
526 Supplementary Figure 2: Phylogenetic tree of the *ROS1* homologous proteins in
527 *Arabidopsis*, tomato and melon.
528 Supplementary Figure 3: RNASeq dataset of *ROS1* melon homologues in the
529 climacteric genotype VED and the non-climacteric genotype "Piel de sapo
530 (PS)".
531 Supplementary Figure 4: Phylogenetic tree of *CTR1* homologous proteins in
532 several plant species
533 Supplementary Figure 5: RNASeq dataset of gene *CmCTR1-like* in the
534 climacteric genotype VED and the non-climacteric genotype "Piel de sapo (PS)"
535 along ripening stages.

536

537 **Acknowledgements**

538 We acknowledge F. Garcia and E. del Blanco for technical support, and K. G.
539 Alexiou for data management.

540

541 **Author contributions**

542
543 Conceptualization: AG, MP and JGM. Investigation and Methodology: AG, MSD
544 and LQ. Writing-Original draft preparation: AG. Writing-Review and editing: AG,
545 MP, MM, JGM, LQ. Supervision: JGM and MM. All authors read and approved
546 the final manuscript.

547
548 **Data availability**
549
550 All available data can be found within manuscript and Supplementary Materials,
551 with further enquiries being directed to the corresponding authors. Bisulfite
552 sequencing data were deposited to European Nucleotide Archive (ENA:
553 <https://www.ebi.ac.uk/ena/browser/home>) with the project accession number
554 PRJEB51881.

555

556 **Conflict of interest**

557 The authors have no conflicts to declare.

558

559 **Funding**

560 This work was supported by Grant RTI2018-097665-B-C2, funded by
561 MCIN/AEI/ 10.13039/501100011033 and by “ERDF A way of making Europe”,
562 Severo Ochoa Programme for Centres of Excellence in R&D CEX2019-000902
563 funded by MCIN/AEI/ 10.13039/501100011033 and the CERCA
564 Programme/Generalitat de Catalunya to J.G.-M. AG was supported by the
565 European Union’s Horizon 2020 research and innovation programme under
566 Marie Skłodowska-Curie (grant agreement No 793090). MSD was supported by
567 a FPI grant from the Spanish Ministry of Economy and Competitiveness BES-
568 2017-079956 funded by MCIN/AEI/ 10.13039/501100011033 and by “ESF
569 Investing in your future”. Work in the Quadrana group is supported by the
570 European Research Council (ERC) under the European Union’s Horizon 2020
571 research and innovation program (grant agreement No. 948674).

572

References

Akalin A, Kormaksson M, Li S, Garrett-Bakelman FE, Figueroa ME, Melnick A, Mason CE. 2012. MethylKit: a comprehensive R package for the analysis of genome-wide DNA methylation profiles. *Genome Biology* **13**, 1–9.

Binder BM. 2008. The ethylene receptors: Complex perception for a simple gas. *Plant Science* **175**, 8–17.

Castelblanque L, Marfa V, Claveria E, I M, L P-G, Dolcet-sanjuan R. 2008. Improving the genetic transformation efficiency of *Cucumis melo* subsp. *melo* “Piel de Sapo” via Agrobacterium. *Transformation*, 627–632.

Chandrasekaran J, Brumin M, Wolf D, Leibman D, Klap C, Pearlsman M, Sherman A, Arazi T, Gal-On A. 2016. Development of broad virus resistance in non-transgenic cucumber using CRISPR/Cas9 technology. *Molecular Plant Pathology*, 1–14.

Cheng J, Niu Q, Zhang B, Chen K, Yang R, Zhu JK, Zhang Y, Lang Z. 2018. Downregulation of RdDM during strawberry fruit ripening. *Genome Biology* **19**.

Doyle, JJ. 1990. Isolation of plant DNA from fresh tissue. *Focus* **12**, 13–15.

Feder A, Jiao C, Galpaz N, et al. 2020. Melon ethylene-mediated transcriptome and methylome dynamics provide insights to volatile production. *bioRxiv*. doi: 10.1101/2020.01.28.923284 [PrePrint]

Feng Z, Mao Y, Xu N, et al. 2014. Multigeneration analysis reveals the inheritance, specificity, and patterns of CRISPR/Cas-induced gene modifications in *Arabidopsis*. *Proceedings of the National Academy of Sciences* **111**, 4632–4637.

Fu DQ, Zhu BZ, Zhu HL, Jiang WB, Luo YB. 2005. Virus-induced gene silencing in tomato fruit. *Plant Journal* **43**, 299–308.

García-Almodóvar RC, Gosálvez B, Aranda MA, Burgos L. 2017. Production of transgenic diploid *Cucumis melo* plants. *Plant Cell, Tissue and Organ Culture (PCTOC)* 2017 130:2 **130**, 323–333.

Giovannoni J. 2001. Molecular biology of fruit maturation and ripening. *Annual review of plant physiology and plant molecular biology* **52**, 725–749.

Giovannoni JJ. 2007. Fruit ripening mutants yield insights into ripening control. *Current Opinion in Plant Biology* **10**, 283–289.

Giovannoni J, Nguyen C, Ampofo B, Zhong S, Fei Z. 2017. The Epigenome and Transcriptional Dynamics of Fruit Ripening. <https://doi.org/10.1146/annurev-arplant-042916-040906> **68**, 61–84.

Gong Z, Morales-Ruiz T, Ariza RR, Roldán-Arjona T, David L, Zhu J-K. 2002. ROS1, a Repressor of Transcriptional Gene Silencing in *Arabidopsis*, Encodes a DNA Glycosylase/Lyase. *Cell* **111**, 803–814.

Halter T, Wang J, Amesefe D, Lastrucci E, Charvin M, Rastogi MS, Navarro L. 2021. The *arabidopsis* active demethylase *ros1* cis-regulates defense genes by erasing dna methylation at promoter-regulatory regions. *eLife* **10**, 1–62.

Hooghvorst I, López-Cristoffanini C, Nogués S. 2019. Efficient knockout of phytoene desaturase gene using CRISPR/Cas9 in melon. *Scientific Reports* 2019 9:1 **9**, 1–7.

Huang H, Liu R, Niu Q, Tang K, Zhang B, Zhang H, Chen K, Zhu JK, Lang Z. 2019. Global increase in DNA methylation during orange fruit development and ripening. *Proceedings of the National Academy of Sciences of the United States of America* **116**, 1430–1436.

Ito Y, Nishizawa-Yokoi A, Endo M, Mikami M, Toki S. 2015. CRISPR/Cas9-mediated mutagenesis of the RIN locus that regulates tomato fruit ripening. *Biochemical and Biophysical Research Communications* **467**, 76–82.

Kieber JJ, Rothenberg M, Roman G, Feldmann KA, Ecker JR. 1993. CTR1, a negative regulator of the ethylene response pathway in *arabidopsis*, encodes a member of the Raf family of protein kinases. *Cell* **72**, 427–441.

Krueger F, Andrews SR. 2011. Bismark: a flexible aligner and methylation caller for Bisulfite-Seq applications. *Bioinformatics* **27**, 1571–1572.

Lang Z, Wang Y, Tang K, Tang D, Datsenko T, Cheng J, Zhang Y, Handa AK, Zhu JK. 2017. Critical roles of DNA demethylation in the activation of ripening-induced genes and inhibition of ripening-repressed genes in tomato fruit. *Proceedings of the National Academy of Sciences of the United States of America* **114**, E4511–E4519.

Le T-N, Schumann U, Smith NA, et al. 2014. DNA demethylases target promoter transposable elements to positively regulate stress responsive genes in *Arabidopsis*. *Genome Biology* 2014 15:9 **15**, 1–18.

Liu R, How-Kit A, Stammitti L, et al. 2015. A DEMETER-like DNA demethylase governs tomato fruit ripening. *Proceedings of the National Academy of Sciences of the United States of America* **112**, 10804–10809.

Lü P, Yu S, Zhu N, et al. 2018. Genome encode analyses reveal the basis of convergent evolution of fleshy fruit ripening. *Nature Plants* **4**, 784–791.

Manning K, Tör M, Poole M, Hong Y, Thompson AJ, King GJ, Giovannoni JJ, Seymour GB. 2006. A naturally occurring epigenetic mutation in a gene encoding an SBP-box transcription factor inhibits tomato fruit ripening. *Nature Genetics* 2006 38:8 **38**, 948–952.

McMurchie EJ, McGlasson WB, Eaks IL. 1972. Treatment of fruit with propylene gives information about the biogenesis of ethylene. *Nature* **237**, 235–6.

Penterman J, Zilberman D, Jin HH, Ballinger T, Henikoff S, Fischer RL. 2007. DNA demethylation in the *Arabidopsis* genome. *Proceedings of the National Academy of Sciences of the United States of America* **104**, 6752–6757.

Pereira L, Pujol M, Garcia-mas J, Phillips MA. 2017. Non-invasive quantification of ethylene in attached fruit headspace at 1 p . p . b . by gas chromatography – mass spectrometry, 172–183.

Pereira L, Ruggieri V, Pérez S, Alexiou KG, Fernández M, Jahrmann T, Pujol M, Garcia-Mas J. 2018. QTL mapping of melon fruit quality traits using a high-density GBS-based genetic map. *BMC Plant Biology* **18**, 1–17.

Pereira L, Santo Domingo M, Ruggieri V, Argyris J, Phillips MA, Zhao G, et al. 2020. Genetic dissection of climacteric fruit ripening in a melon population segregating for ripening behavior. *Horticulture Research* **7**, 1–18.

R Core Team. 2020. A Language and Environment for Statistical Computing.

RStudio: Integrated development environment for R. 2012. Boston, MA, USA: RStudio Inc.

Ruggieri V, Alexiou KG, Morata J, et al. 2018. An improved assembly and annotation of the melon (*Cucumis melo* L.) reference genome. *Scientific reports* **8**.

Schiml S, Puchta H. 2016. Revolutionizing plant biology: multiple ways of genome engineering by CRISPR / Cas. *Plant Methods*, 1–9.

Tian S, Jiang L, Cui X, et al. 2018. Engineering herbicide-resistant watermelon variety through CRISPR/Cas9-mediated base-editing. *Plant Cell Reports* 2018 37:9 **37**, 1353–1356.

Tian S, Jiang L, Gao Q, et al. 2016. Efficient CRISPR/Cas9-based gene knockout in watermelon. *Plant Cell Reports* 2016 36:3 **36**, 399–406.

Vrebalov J, Ruezinsky D, Padmanabhan V, White R, Medrano D, Drake R, Schuch W, Giovannoni J. 2002. A MADS-box gene necessary for fruit ripening at the tomato ripening-inhibitor (*rin*) locus. *Science* **296**, 343–346.

Wang R, Angenent GC, Seymour G, de Maagd RA. 2020. Revisiting the Role of Master Regulators in Tomato Ripening. *Trends in Plant Science* **25**, 291–301.

Yamamoto C, Miki D, Zheng Z, Ma J, Wang J, Yang Z, Dong J, Zhu J-K. 2014. Overproduction of stomatal lineage cells in *Arabidopsis* mutants defective in active DNA demethylation. *Nature Communications* 2014 5:1 **5**, 1–7.

Zhong S, Fei Z, Chen YR, et al. 2013. Single-base resolution methylomes of tomato fruit development reveal epigenome modifications associated with ripening. *Nature Biotechnology* **31**, 154–159.

Zhu JK. 2009. Active DNA demethylation mediated by DNA glycosylases. *Annual Review of Genetics* **43**, 143–166.

573 **Figure Legends:**

574 **Figure 1:** Schematic representation of the target sites for CRISPR/Cas9 and
575 selected CRISPR edited lines. **(A)** Position of the gRNA target sites (red
576 triangle) and selected mutations in the CRISPR lines for *CmROS1* **(B)** Position
577 of the gRNA target sites (red triangle) and selected mutations in the CRISPR
578 lines for *CmCTR1*-like **(C)** Fruit phenotype at harvest time of the wild type VED
579 and CRISPR edited lines.

580

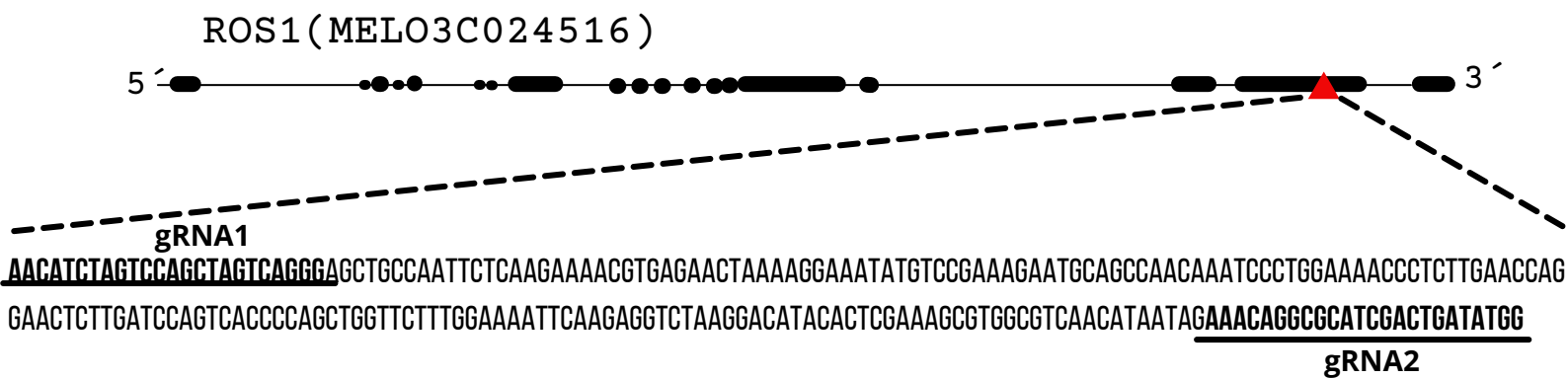
581 **Figure 2:** Evaluation of climacteric ripening associated traits in CRISPR edited
582 lines and VED (in two consecutive years) and ethylene emission rates. **(A)**
583 Earliness of chlorophyll degradation (ECD), Earliness of production of aroma
584 (EARO) and Earliness of abscission layer formation (EALF) in 2020 **(B)** ECD,
585 EARO and EALF in 2021. Means followed by different letters differ significantly
586 (T-test, $p<0.05$) **(C)** Ethylene production in attached fruits from 25 days after
587 pollination (DAP) until harvest in 2020.

588

589 **Figure 3:** General methylation and DMR regions at different ripening stages
590 (15, 25, 30 DAP and (H) Harvest point) of VED and CRISPR-ROS1 line. **(A)**
591 Fruit ripening stages **(B)** number of DMRs along ripening in VED **(C)** number of
592 DMRs in VED vs CRISPR-ROS1 at the same time point of ripening **(D)** DMRs
593 annotation in VED along ripening **(E)** DMRs annotation in VED vs CRISPR-
594 ROS1 at the same time point of ripening. DMRs were detected using Fisher's
595 exact test and applying a Benjamin-Hochberg (BH) adjusted statistical threshold
596 (FDR 0.05). Only DMRs with DNA methylation changes of 40%, 20% and 20%
597 for CG, CHG and CHH context, respectively were consider.

598

599 **Figure 4:** DNA methylation levels of ethylene related genes and ripening
600 associated transcription factors for VED and CRISPR-ROS1 at different fruit
601 ripening development stages in the three contexts **(A)** *ACO1* in CHH context at
602 25 (left) and 30 DAP (right) **(B)** *ACS1* in CHG context at 25 (left) and 30 DAP
603 (right) **(C)** *ETR1* in CHG context at 30 DAP **(D)** ripening associated transcription
604 factors in CHH context: *NAC-NOR* at 30 DAP, *RIN* at Harvest (H) point and
605 *CNN* at Harvest (H) point.

A**B**

CTR1-like (MELO3C024518)

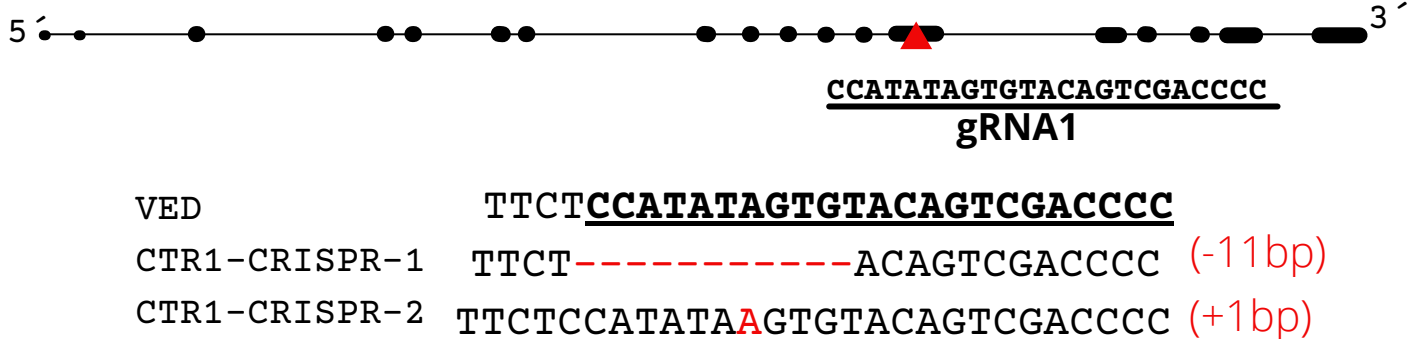
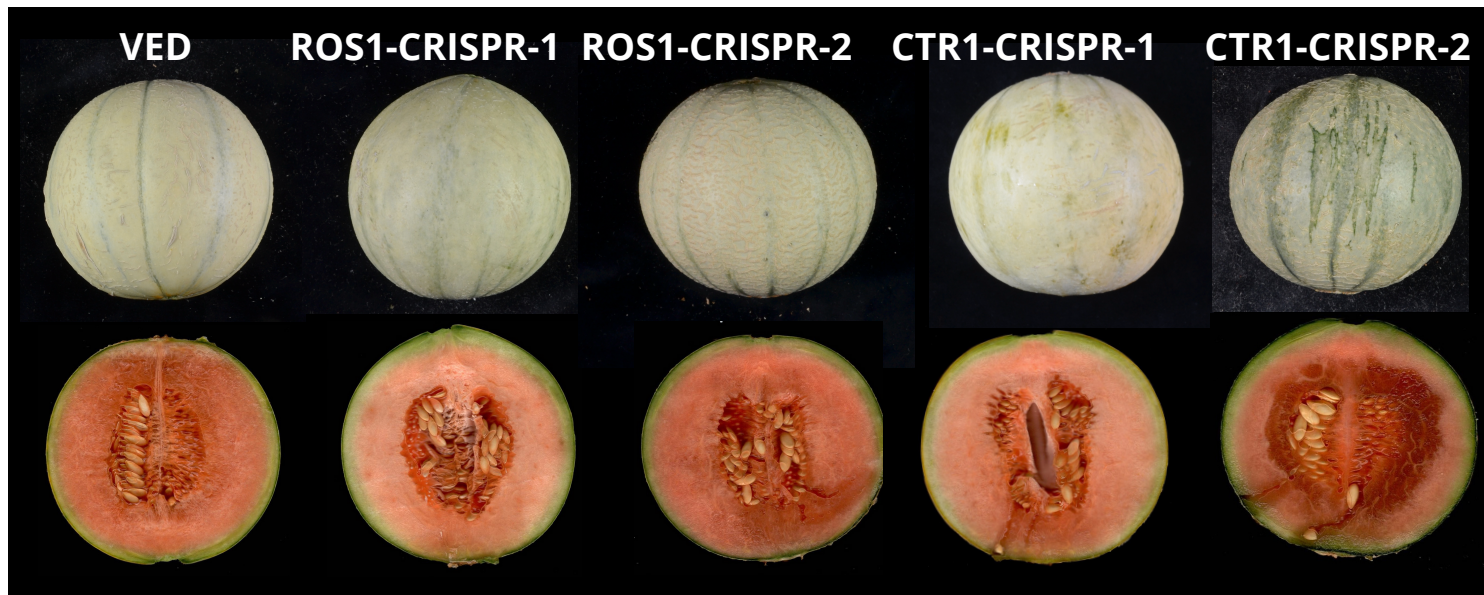
**C**

Figure 1: Schematic representation of the target sites for CRISPR/Cas9 and selected CRISPR edited lines. (A) Position of the gRNA target sites (red triangle) and selected mutations in the CRISPR lines for CmROS1(B) Position of the gRNA target sites (red triangle) and selected mutations in the CRISPR lines for CmCTR1-like (C) Fruit phenotype at harvest time of the wild type VED and CRISPR edited lines.

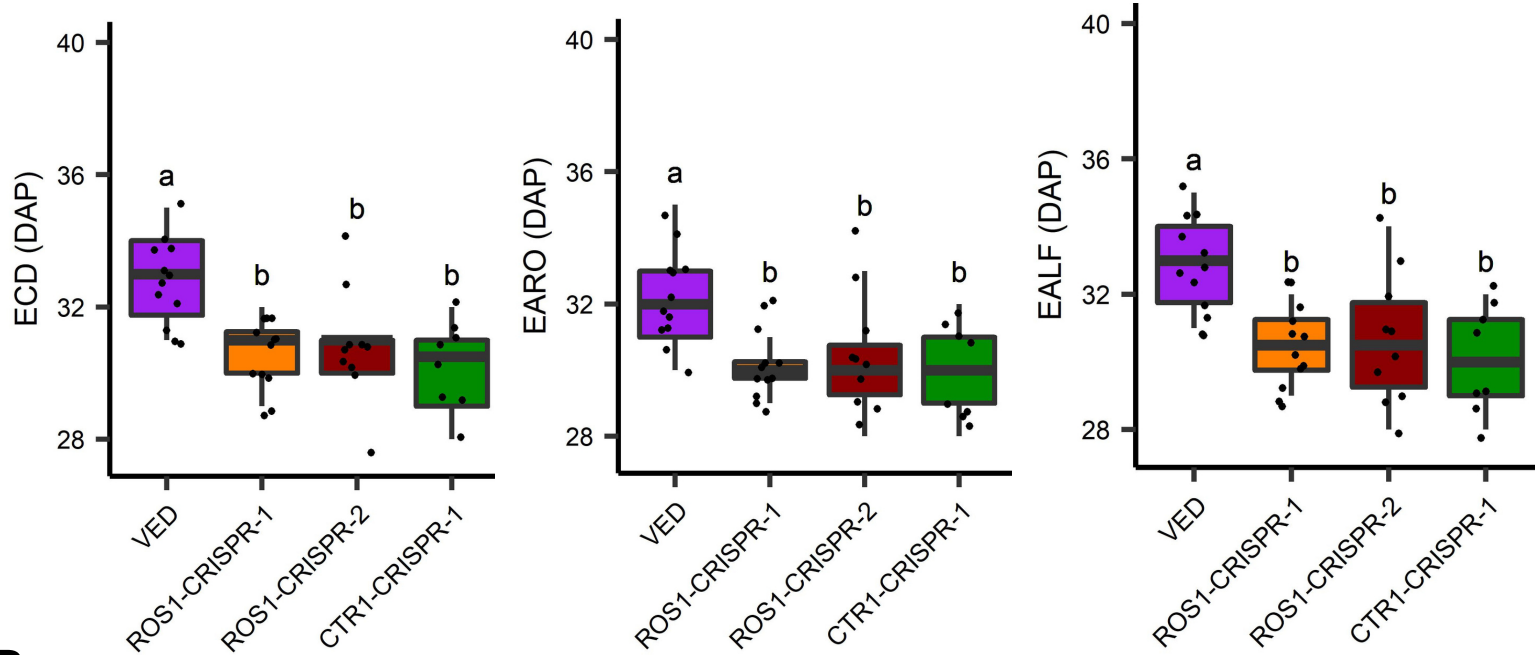
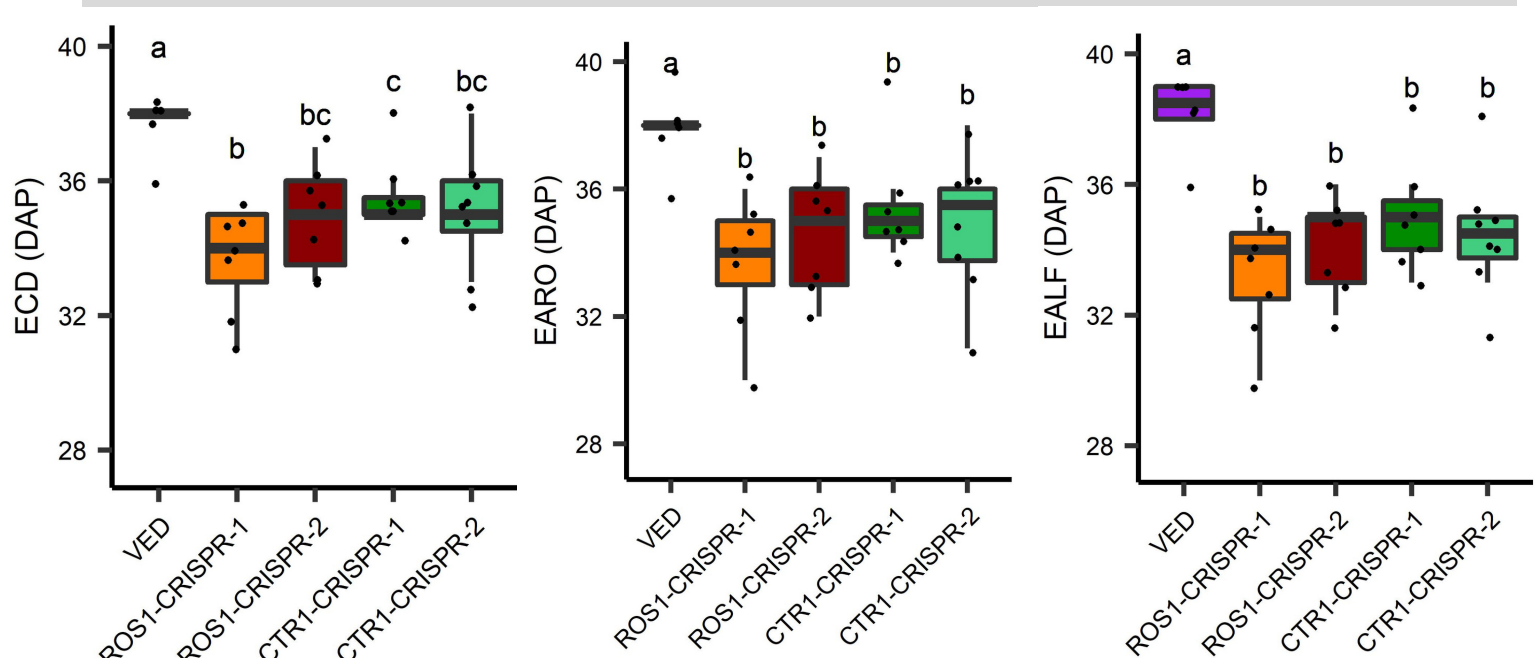
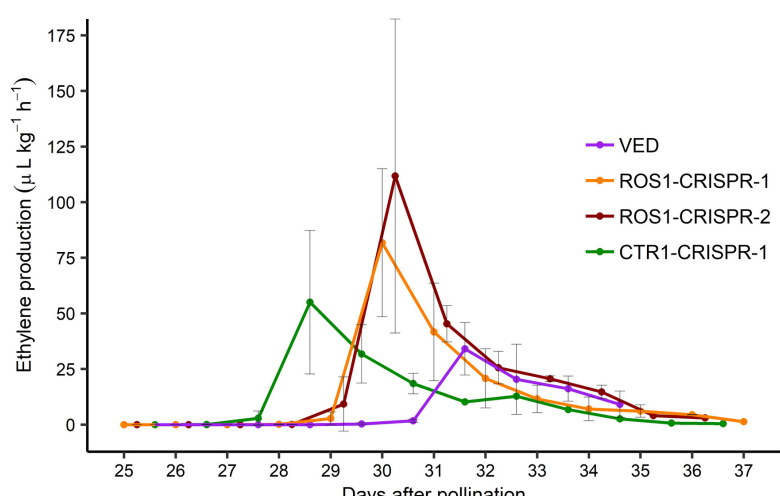
A**Summer season 2020****B****Summer season 2021****C**

Figure 2: Evaluation of climacteric ripening associated traits in CRISPR edited lines and VED (in two consecutive years) and ethylene emission rates. (A) Earliness of chlorophyll degradation (ECD), Earliness of production of aroma (EARO) and Earliness of abscission layer formation (EALF) in 2020 (B) ECD, EARO and EALF in 2021. Means followed by different letters differ significantly (Tukey test, $p < 0.05$) (C) Ethylene production in attached fruits from 25 days after pollination (DAP) until harvest in 2020.

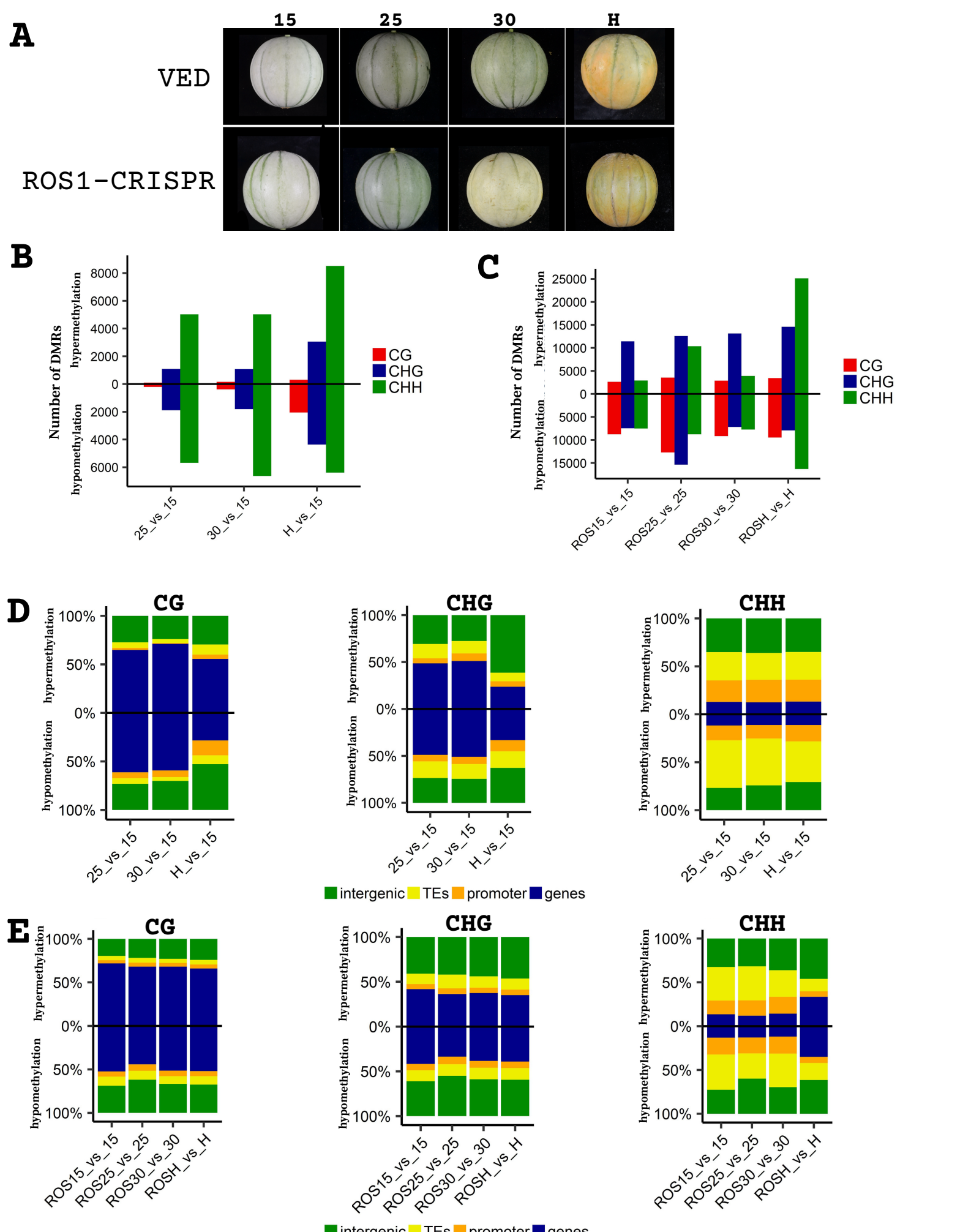
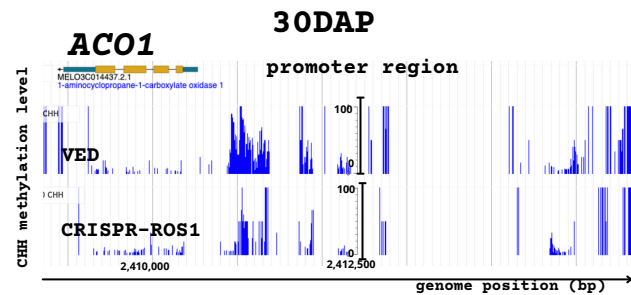
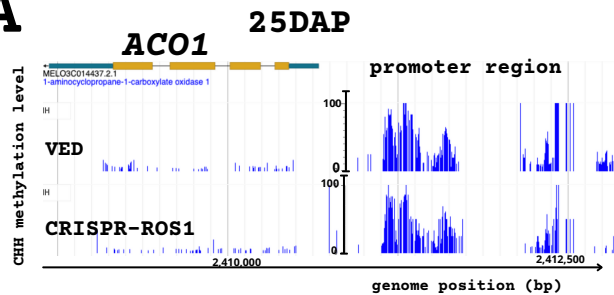


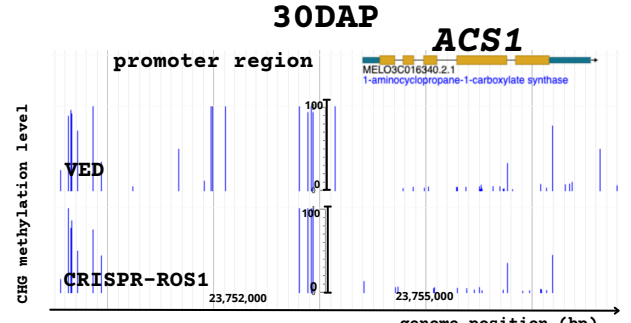
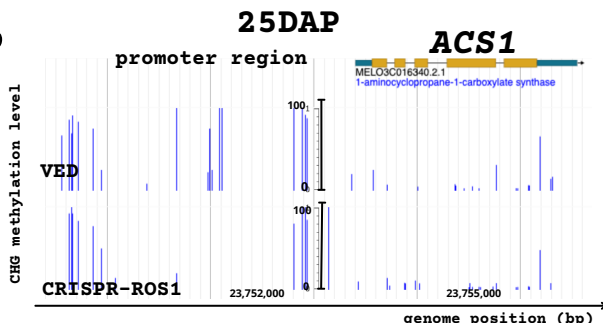
Figure 3: General methylation and DMR regions at different ripening stages (15, 25, 30 DAP and (H) Harvest point) of VED and CRISPR-ROS1 line. (A) Fruit ripening stages (B) number of DMRs along ripening in VED (C) number of DMRs in VED vs CRISPR-ROS1 at the same time point of ripening (D) DMRs annotation in VED along ripening (E) DMRs annotation in VED vs CRISPR-ROS1 at the same time point of ripening. DMRs were detected using Fisher's exact test and applying a Benjamin-Hochberg (BH) adjusted statistical threshold (FDR 0.05). Only DMRs with DNA methylation changes of 40%, 20% and 20% for CG, CHG and CHH context, respectively were considered.

Ethylene related genes

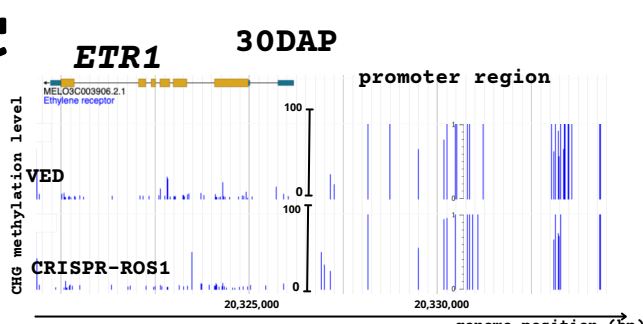
A



B

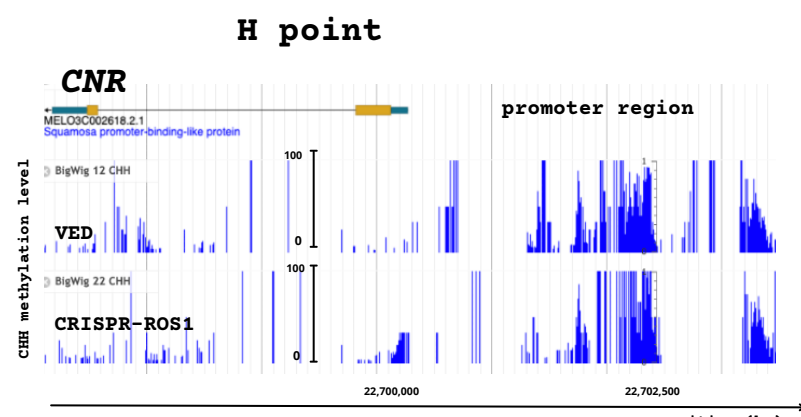
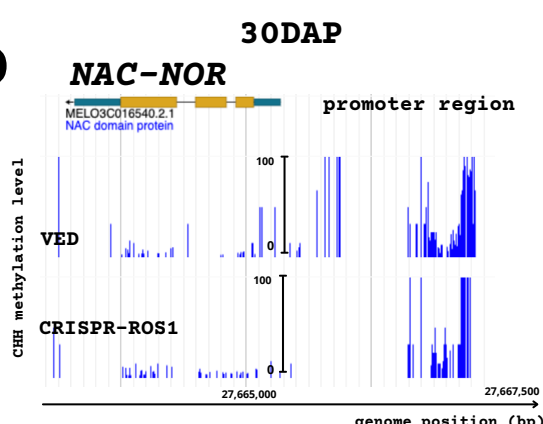


C



Ripening associated TF

D



H point RIN

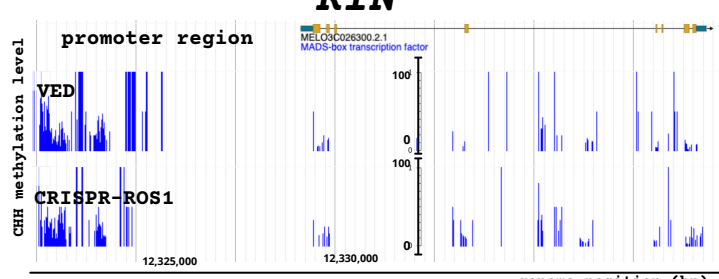


Figure 4: DNA methylation levels of ethylene related genes and ripening associated transcription factors for VED and CRISPR-ROS1 in different fruit ripening development stages in the three contexts (A) ACO1 in CHH context at 25 (left) and 30 DAP (right) (B) ACS1 in CHG context at 25 (left) and 30 DAP (right) (C) ETR1 in CHG context at 30 DAP (D) ripening associated transcription factors in CHH context: NAC-NOR at 30 DAP, RIN at H (Harvest) point and CNN at H (Harvest) point.